

A local metallic state in globally insulating $La_{1.24}Sr_{1.76}Mn_2O_7$ well above the metal-insulator transition

Z. Sun,^{1,2,*} J. F. Douglas,¹ A. V. Fedorov,² Y. -D. Chuang,² H. Zheng,³ J. F. Mitchell,³ and D. S. Dessau^{1,†}

¹Department of Physics, University of Colorado, Boulder, CO 80309, USA

²Advanced Light Source, Lawrence Berkeley National Laboratory, Berkeley, CA 94720, USA

³Materials Science Division, Argonne National Laboratory, Argonne, IL 60439, USA

(Dated: February 6, 2008)

In the spectacularly successful theory of solids, the distinction between metals, semiconductors, and insulators is based upon the behavior of the electrons nearest the Fermi level E_F , which separates the occupied from unoccupied electron energy levels. A metal has E_F in the middle of a band of electronic states, while E_F in insulators and semiconductors lies in the gap between states. The temperature-induced transition from a metallic to an insulating state in a solid is generally connected to a vanishing of the low energy electronic excitations¹. Here we show the first direct evidence of a counter example, in which a significant electronic density of states at the Fermi energy exists in the insulating regime. In particular, angle-resolved photoemission data from the “colossal magnetoresistive” oxide $La_{1.24}Sr_{1.76}Mn_2O_7$ show clear Fermi edge steps both below the T_C when the sample is globally metallic, as well as above T_C when it is globally insulating. Further, small amounts of metallic spectral weight survive up to the temperature scale T^* more than twice the T_C of the system. Such behavior also may have close ties to a variety of exotic phenomena in correlated electron systems including in particular the pseudogap scale T^* in underdoped cuprates².

As shown in figure 1a, the colossal magnetoresistive (CMR) oxide $La_{2-2x}Sr_{1+2x}Mn_2O_7$ ($x=0.38$) exhibits a metal insulator transition at a T_C of about 130K, at which point the system also switches from being a ferromagnet (low T) to a paramagnet (high T)³. We performed angle-resolved photoemission spectroscopy (ARPES) experiments on cleaved single crystals of these materials, with an experimental arrangement as described elsewhere⁴. ARPES is an ideal experimental probe of the electronic structure since it gives the momentum-resolved single-particle excitation spectrum. As discussed in ref. 4 the $x=0.38$ compound studied here does not contain the low energy pseudogap of the $x=0.4$ samples^{5,6,7,8} (see supplementary material for more details on this, the possible issue of surface sensitivity of ARPES, and of possible intergrowths at the surface). The much larger metallic spectral weight of these non-pseudogapped compounds also allows us to study the electronic behavior in greater detail.

Figure 1c shows a large-energy-scale experimental picture of a low temperature $d_{x^2-y^2}$ symmetry band taken

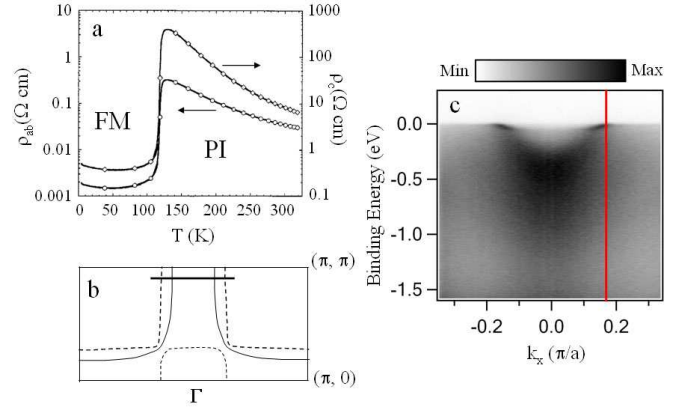


FIG. 1: Overview of features of $La_{1.24}Sr_{1.76}Mn_2O_7$. (a) Resistivity vs. temperature, after ref 3. (b) A representative Fermi surface. (c) Low temperature (20K) ARPES data over a large-energy-scale taken along the black cut near the zone boundary, as shown in (b).

along the black cut near the zone boundary, as shown in figure 1b. We are able to get clean data by isolating the various bilayer-split bands using different photon energies, as described in ref. 4. In particular, in this paper we only show data from the antibonding bilayer-split band which has Fermi crossings at $k_x = \pm 0.17 \pi/a$, $k_x = 0.9 \pi/a$, corresponding to the solid Fermi surface in figure 1b. The energy distribution curves (EDCs) at k_F (indicated by the red line in figure 1c) taken at a series of temperatures are shown in figure 2a. Figure 2b shows the identical spectra and identical scaling, but offset vertically for clarity. All spectra have been normalized only to the incident photon flux.

At low temperature, the EDCs clearly show a structure of peak-dip-hump, where the peak and the hump would nominally be considered the coherent part (quasiparticle) and “incoherent” part of the single particle spectrum respectively, as has been discussed for the spectra of the high T_C cuprate superconductors^{9,10,11}. One sees that the near- E_F spectral weight diminishes with increasing temperature, while the high binding energy (>700 meV) part is less affected by temperature. Contrary to the general picture of the metal-insulator transition, in which a gap develops in the single particle spectrum when an electronic system becomes insulating¹, the EDCs here still exhibit a sharp Fermi cutoff indicating metallic behavior.

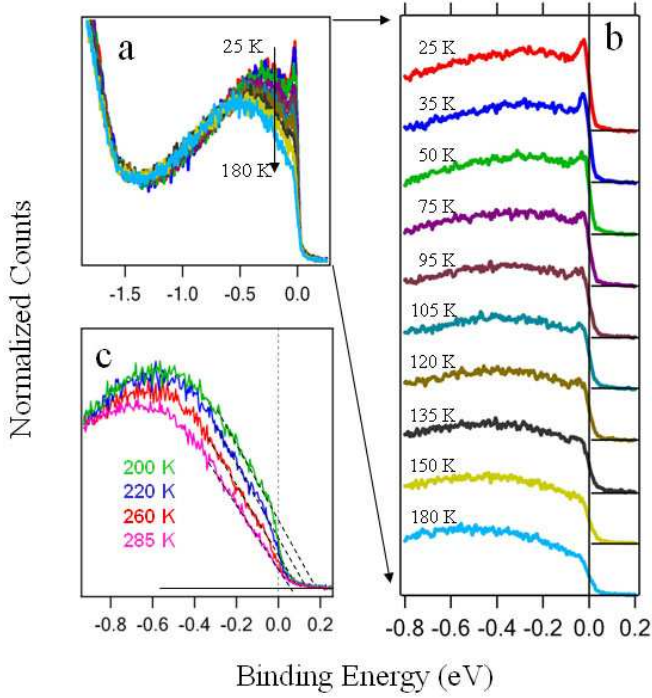


FIG. 2: Energy Distribution Curves (EDCs) as a function of temperature at k_F (red line of figure 1c), indicating metallic spectral weight above T_C . (a, b) the same data set scaled by the incident flux and are taken while warming. (c) EDCs from a different sample taken at the high temperature range. Clear breaks are seen in the spectral intensity near E_F for all but the highest temperature, indicating finite metallic spectral weight and a T^* just above 285K (see figure 3 for details of the T^* determination).

ior at temperatures in which the macroscopic DC conductivity is characteristic of insulation (e.g. the spectra at 135, 150 and 180K). To our knowledge, this unusual behavior, a metallic Fermi edge in a globally insulating system, has not been previously observed on the insulating side of a metal-insulator transition. The opposite, in which a metallic system shows a lack of a Fermi cutoff, is on the other hand expected in exotic low-dimensional systems such as the Luttinger Liquids¹², and has likely been observed¹³. The other situation most likely to show a metallic Fermi edge in a globally insulating system is that of an Anderson-localized system beyond the mobility edge. However, in such systems a Coulomb gap is expected to remove the metallic weight near the Fermi energy¹⁴. Our data could only be consistent with such a scenario if the Coulomb gap were extremely small - on the order of a few meV or less. Such a picture also would not naturally explain the metallic spectral weight dependence with temperature, to be discussed in more detail later in the letter.

On a different sample we have done higher temperature scans, looking for a possible temperature scale at which the metallic spectral weight disappears. These data are

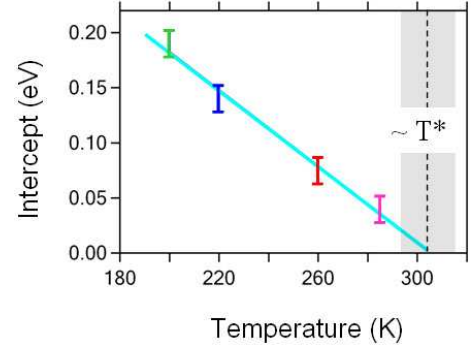


FIG. 3: Determination of T^* . Zero intensity intercepts as a function of temperature from the linear fits to the data shown in figure 2c. These intercepts go to zero at 305K, which we label as $T^* \sim 305\text{K}$.

shown in figure 2c and show a clear discontinuity in the slope near the Fermi energy for all but the 285K data, indicating a finite metallic spectral weight. This effect is emphasized by an extrapolation of the spectral weight using a simple linear fit to the data between -0.3 and -0.05 eV, as shown by the dotted lines in the figure. Upon raising the sample temperature we see that the intercept of these dotted lines with the horizontal axis decreases at an approximately linear rate (figure 3). As shown in this figure these zero intensity intercepts reach the Fermi energy at $305 \pm 10\text{K}$. We thus indicate 305K as the temperature at which the first bits of metallic weight become apparent, which we indicate as the temperature T^* . Technical reasons including sample aging and excessive manipulator drift preclude us from making the full range of measurements on a single cleave. We therefore used different samples to study the electronic excitations in different temperature regimes.

Figure 4a shows the electronic dispersion of the near-Fermi states as a function of temperature obtained from an analysis of momentum distribution curves (MDCs). This data indicates that the main properties of the metal, such as the Fermi wave vector k_F , the Fermi velocity v_F , the electron phonon coupling parameter λ , and the effective mass m^* don't change significantly as a function of temperature, even as the metal-insulator transition temperature T_C is traversed. This is an unexpected behaviour for a metal-insulator transition in which these parameters would vary dramatically with temperature, and likely even diverge¹.

Our data can be understood by invoking a model of disconnected local ferromagnetic metallic regimes above T_C up to approximately the temperature T^* . This suggestion is consistent with earlier studies which have found significant ferromagnetic signals far above T_C ^{15,16,17,18}, since metallicity and ferromagnetism should have a connection in these systems via the double-exchange interaction. In general, the metallic regions may be either phase separated (and possibly static) domains^{19,22} or they may

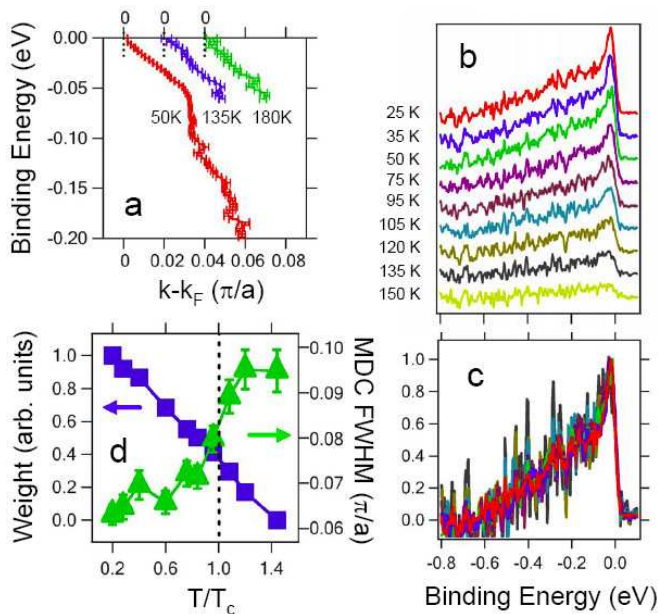


FIG. 4: Properties of the metallic portion of the sample. (a) Electronic dispersion showing a similar k_F , v_F and electron-phonon coupling as a function of temperature. (b, c) Metallic EDCs or M-EDCs obtained by subtracting the 180K EDC from all lower temperature data. (b) shows the raw scaling while (c) scales each spectrum to have a similar max intensity. (d) MDC widths (green triangles) and integrated M-EDC spectral weights (blue squares) as a function of temperature.

be dynamic fluctuations of the ferromagnetic metallic state, which in a two-dimensional system may persist to quite high temperatures^{15,16,17,18}. We will discuss these two possibilities later in this letter. Here we show that we can study the metallic portions further by our ability to approximately deconvolve the spectrum into the components which arise from the metal and non-metal portions. We do this by subtracting the 180K EDC from all other EDCs as shown in figure 2b to create “metallic EDCs” or M-EDCs as shown in figure 4b. It should be pointed out that the slight variation of spectra from sample to sample, which has been commonly observed in ARPES, imperils the practice of extracting data of one sample from that of another. Therefore, we don’t use the higher temperature data of figure 2c to do the subtraction as this is from a different sample. Figure 4c shows the same M-EDCs but scaled to all have the same amplitude. Within the noise, all the M-EDCs have similar lineshapes with coherent peaks near E_F and an incoherent background at high binding energy, though the widths of the M-EDC coherent peak (or low energy MDC peak) become broader with increasing temperature (figure 4d). The integrated spectral weight of the M-EDCs varies smoothly as a function of temperature, with no clear break at T_C (figure 4d). This, as well as the approximate temperature-independence of the M-EDC

lineshape indicates that the electrons in the metallic regions have similar properties above and below T_C , and that temperature has surprisingly little effect on the behavior or interactions of electrons in the metallic regions. This is consistent with the approximate independence of v_F , λ , and m^* in the metallic regions shown in figure 4a. The experimentally determined MDC width of the electrons at the Fermi energy (green triangles of figure 4d) does broaden with increasing temperature. The inverse of this quantity, the mean free path of the electrons, thus decreases with increasing temperature, consistent with a decreased size of metallic regions or increased scattering events at higher temperatures.

While many aspects of our data are consistent with either the phase separation or magnetic fluctuation picture, certain aspects of it can address the question of whether the metallic regions above T_C are phase-separated out from a more insulating environment^{19,20}, or if they are just fluctuations from a lower temperature ordered environment which is otherwise homogeneous^{17,18}. In particular, the smooth dependence of the spectral weight of the metallic regions as a function of temperature across T_C (blue squares of figure 4d) is more consistent with phase separation, as we would likely expect a clear drop in the metallic weight near T_C if the metallic portions were just fluctuations of the ordered lower temperature environment. At other doping levels (for example $x=0.4$), experiments do observe a sharp drop in the metallic weight at T_C to zero or almost zero⁸, and so those samples may be more consistent with the fluctuation physics.

Within the picture of phase separation, we imagine that the metallic islands arise at a temperature T^* near room temperature, which also may be related to the temperature scale at which polaronic correlations freeze²¹. As the temperature is lowered the size and proportion of metallic portions grows until a critical ratio of metallic to insulating portions is reached. At that point electrons can percolate from one metallic region to another, bringing about the macroscopic metallic¹⁹ and ferromagnetic states, as well as being consistent with the “colossal” decrease in resistivity with an applied magnetic field. In certain models this behavior is expected from a competition between different phases, for example between the ferromagnetic metal phase and the charge-ordered antiferromagnetic insulating phase^{19,22,23}, though in contrast to ref 19, the materials used here are far away from the charge-ordered doping level. Theoretical arguments predict both the phase separation and the existence of a higher temperature scale T^{*24} , with ideas similar to the Griffiths singularity²⁵ in which T^* would be the critical temperature of the associated clean system in the absence of disorder, and which have recently been discussed in the context of manganite physics^{24,26}. We are presently undertaking a more thorough study of the full Fermi surface to test this percolation model quantitatively.

A T^* scale is one of the key properties of the high T_C superconductors, and has for years been the subject of intense controversy². In these compounds, disorder also

appears to be highly relevant, especially in the underdoped regime where the T^* scale exists. In that case it signals the emergence of the pseudogap, which may be the precursor to the long range superconducting order which forms at T_C ²⁷ – a clear analogy to the manganites where T^* signals the emergence of the metallic domains which become long range at T_C . Also similar to the cuprates, it appears that the T^* temperature scales may not be universal to all doping levels of the manganites. Pinning these details down and then understanding their implications will certainly be an area of intense study in the near future.

It is becoming increasingly clear that some of the most dramatic responses in modern materials occur in systems in which multiple phases or orders with similar energy scales compete with each other^{22,23,24,28}. It is then natural that in at least some of these systems spatial heterogeneities will occur, and small perturbations can cause drastic macroscopic alterations to the physical properties or even new types of “emergent” behavior. The key is finding which aspects of the inhomogeneity are intrinsic

and what is their role in determining the key physical properties of the system.

The authors thank Y. Tokura and T. Kimura for providing preliminary samples and are grateful to D. N. Argyriou, A. Bansil, E. Dagotto, K. Gray, A. Moreo, R. Osborn, L. Radzihovsky, D. Reznik, S. Rosenkranz, Y. Tokura, and M. Veillette for helpful discussions. This work was supported by the U.S. Department of Energy under grant DE-FG02-03ER46066 and by the U.S. National Science Foundation grant DMR 0402814. The ALS is operated by the Department of Energy, Office of Basic Energy Sciences. Argonne National Laboratory, a U.S. Department of Energy Office of Science Laboratory, is operated under Contract No. DE-AC02-06CH11357. The U.S. Government retains for itself, and others acting on its behalf, a paid-up nonexclusive, irrevocable worldwide license in said article to reproduce, prepare derivative works, distribute copies to the public, and perform publicly and display publicly, by or on behalf of the Government.

* zsun@lbl.gov

† Dessau@colorado.edu

- ¹ M. Imada, A. Fujimori, and Y. Tokura, Rev. Mod. Phys. **70**, 1039 (1998).
- ² T. Timusk and B. Statt, Rep. Prog. Phys. **62**, 61 (1999).
- ³ Q. A. Li, et al., Phys. Rev. B **59**, 9357 (1999).
- ⁴ Z. Sun et al., Phys. Rev. Lett. **97**, 056401 (2006).
- ⁵ D. S. Dessau et al., Phys. Rev. Lett. **81**, 192 (1998).
- ⁶ Y.-D. Chuang et al., Science **292**, 1509 (2001).
- ⁷ T. Saitoh et al., Phys. Rev. B **62**, 1039 (2000).
- ⁸ N. Mannella et al., Nature **438**, 474 (2005).
- ⁹ D. S. Dessau et al., Phys. Rev. Lett. **66**, 2160 (1991).
- ¹⁰ Z. -X. Shen and D. S. Dessau, Phys. Rep. **253**, 1 (1995).
- ¹¹ A. Damascelli, Z. Hussain, and Z. -X. Shen, Rev. Mod. Phys. **75**, 473 (2003).
- ¹² J. Voit, Rep. Prog. Phys. **57**, 977 (1995).
- ¹³ J.W. Allen, Sol. State Comm. **123**, 469 (2002).
- ¹⁴ C.M. Varma, Phys. Rev. B **54**, 7328 (1996).
- ¹⁵ D. N. Argyriou, et al., J. Appl. Phys. **83**, 6374 (1998).
- ¹⁶ R. Osborn, et al., Phys. Rev. Lett. **81**, 3964 (1998).
- ¹⁷ S. Rosenkranz, et al., cond-mat/9909059.
- ¹⁸ S. Rosenkranz, et al., Physica B **312-313**, 763-765 (2002).
- ¹⁹ M. Uehara, et al., Nature **399**, 560 (1999).
- ²⁰ E. Dagotto, Nanoscale Phase Separation and Colossal Magnetoresistance (Springer Verlag, 2003).
- ²¹ D.N. Argyriou, et al., Phys. Rev. Lett. **89**, 36401 (2002).
- ²² E. Dagotto, Science **309**, 257 (2005).
- ²³ Y. Tokura, Rep. Prog. Phys. **69**, 797 (2006).
- ²⁴ J. Burgi, et al., Phys. Rev. Lett. **87**, 277202 (2001).
- ²⁵ R.B. Griffiths, Phys. Rev. Lett. **23**, 17 (1969).
- ²⁶ M. B. Salamon, et al., Phys. Rev. Lett. **88**, 197203 (2002).
- ²⁷ V.J. Emery, and S.A. Kivelson, Nature **374**, 434 (1995).
- ²⁸ S. Murakami, and N. Nagaosa, Phys. Rev. Lett. **90**, 197201 (2003).

Supplementary discussion:

1. *The difference between $x=0.38$ and $x=0.4$ samples.*

It should be pointed out that there is a remarkable difference between the ARPES spectra of $La_{1.24}Sr_{1.76}Mn_2O_7$ and $La_{1.2}Sr_{1.8}Mn_2O_7$ samples, even though many macroscopic properties are similar. Quasiparticles have been found near the zone boundary at the doping levels of $x=0.36$ and 0.38 in $La_{2-2x}Sr_{1+2x}Mn_2O_7$, while there exists a large energy pseudogap in $x=0.40$ samples^{4,5,6,7,8}. Temperature dependent studies have also been performed on $x=0.4$ samples and have not shown evidence for metallic spectral weight above T_C ^{6,7,8}. Similar to high- T_C cuprates, physical properties exhibit strong variations with doping in manganites. The cause of the difference between $La_{2-2x}Sr_{1+2x}Mn_2O_7$ ($x=0.38$) and $La_{2-2x}Sr_{1+2x}Mn_2O_7$ ($x=0.40$) samples is not understood yet, though it could have to do with the increased lattice anomalies for the 0.4 samples [J. Mitchell et al., J. Phys. Chem. B **105**, 10731 (2001).], the onset of spin canting between ferromagnetic layers which starts at the doping level of 0.4 [M.Kubota et.al., J. Phys. Soc. Jpn **69**, 1606 (2000).], or even something extrinsic such as a surface issue.

2. *The issue of surface sensitivity.* Because of the shallow probing depth of the ARPES experiment (~ 5 -10 Angstroms), we cannot completely rule out the potential that a surface phase whose properties do not follow those of the bulk gives rise to some of the phenomena reported here. For ARPES on the layered manganites we are relatively well off since the samples cleave readily between the $La, Sr - O$ bilayers, which are ionically (not covalently) bonded. High quality LEED pictures without any evidence of surface reconstruction are obtained from these surfaces. The doping level at the surfaces, as obtained from the Fermi surface volume also appears to be

correct for these samples - for example the $d_{x^2-y^2}$ bonding band Fermi surface nesting vector of $0.27 \times (2\pi/a)$ for the $x = 0.38$ samples used in this study⁴ exactly matches that obtained from neutron scattering measurements²¹. The nesting vector of 0.4 samples is slightly larger at $0.3 \times (2\pi/a)$ ⁶ and also matches the results of scattering measurements [L. Vasiliiu-Doloc, et al. Phys. Rev. Lett. 83, 4393 (1999).].

3. *The issue of intergrowths.* One should consider whether it might be possible for the metallic spectral weight far above T_C to have originated from small bits of intergrowth (IG) of a higher T_C sample left near the surface after cleaving. Here we discuss why that is inconsistent with our data. Such intergrowths should not arise from a layered manganite, as the maximum temperature at which bulk metallic behavior is found among all

known layered manganites is $\sim 160\text{K}$. A small amount of (non-layered) perovskite-like IG with a $T_C = 300\text{K}$ could exist at a cleaved surface, though would not show the bilayer splitting since the perovskite samples have only one MnO_2 plane per unit cell. Both our high and low temperature data display this bilayer band splitting (this paper only presents the data from the antibonding component), which is a direct consequence of having two MnO_2 planes per unit cell. In addition to being able to vary the intensity of the bilayer split bands (relative and overall) by taking advantage of the photoemission matrix elements, we can follow the dispersion in E and k of each of the bilayer bands, including tracking them all the way to E_F . Therefore we know the origin of the metallic weight as explicitly originating from these bilayer split bands, and therefore, from the bilayer manganite.